Asymmetric relief of surface stress induced by a chiral adsorbate: Alaninate adsorption on Cu(110)

M. Blanco-Rey* and G. Jones†
Department of Chemistry, University of Cambridge, Lensfield Road, Cambridge CB2 1EW, United Kingdom
(Received 18 March 2010; revised manuscript received 26 April 2010; published 19 May 2010)

Using first-principles calculations, we explore symmetry breaking in the surface stress tensor induced upon adsorption of chiral species on an achiral metallic substrate, namely, alaninate on Cu(110). The stress sensitivity to coverage and adsorption geometry is studied in the known (2×3) phase and other related reconstructions. We find that alaninate relieves stress in the Cu(110) surface by electron transfer from the substrate to the molecule. In a low coverage regime, $\Theta=1/6$, the principal stresses are found to deviate in opposite directions by an angle $\alpha\sim15°$ from the substrate mirror plane directions, $[1\bar{1}0]$, depending on the chirality of the alaninate adsorption footprint. In medium-high coverage regimes, $\Theta\geq0.3$, the observed asymmetries are weaker, consistent with the presence of H bonds lying close to $[1\bar{1}0]$. The studied $\Theta=1/3$ enantiopure models show the same asymmetry orientation with $\alpha\sim5°$. Thus, stress relief anisotropy is diagnostic of the molecular chirality in this case. We also find that the substrate intrinsic tensile stress is relieved at $\Theta\gtrsim0.25$, when the adsorbates form the onset of a H-bound network. At higher coverages, the system is under net compressive stress.

DOI: 10.1103/PhysRevB.81.205428 PACS number(s): 68.43.Fg, 68.43.Hn, 68.03.Cd

I. INTRODUCTION

Surface stress is a fundamental property that appears at surfaces in equilibrium and has its origin in the strength of surface bonds.[1–3] Metal surfaces are under tensile stress, as determined from density-functional-theory (DFT)-based calculations.[4–9] Although no experimental technique has been implemented yet to measure this intrinsic or absolute surface stress, it is already possible to measure stress changes associated to relaxations and charge rearrangement during adsorption of molecules and thin films.[2,10–14] In the low-coverage regime stress depends linearly on the coverage, Θ. At high coverages, such that adsorbates interact strongly (by orbital overlap), dependence switches to exponential, as $\propto e^{-c/\sqrt{\Theta}}$, where c is a constant.[10] Weakly interacting adsorbates (e.g., dipole-mediated interactions) yield smaller stress contributions.

Experimental methods, usually based in cantilever bending, are sensitive to surface stresses as small as 0.01 N/m $(6.24\times10^{-4}$ eV Å$^{-2})$.[13,14] Not only atomic and CO adsorption induced stresses have been probed in this way[2] but also larger molecules forming self-assembled monolayers (SAMs), such as alkanethiols on gold.[15] The latter case shows a compressive surface stress change within the linear regime during the self-assembly process with subtle stress oscillations attributed to intermolecular dipole interactions.[16] DFT shows that this compressive stress is due to charge transfer from localized bonds in the surface into the Au-S bond.[16] Thus, the surface stress relief is a reflection of the nature of both the adsorbate-substrate and the adsorbate-adsorbate bonding. We introduce another relevant case study: SAMs with chiral properties on metal substrates, where chirality will manifest itself as an asymmetry in the surface stress tensor that can be quantified from DFT.[17] The experimental setups and post processing can be upgraded to measure anisotropic stresses.[18–21] However, determination of the stresses along arbitrary directions on a sample remains as a technical challenge.

In the present paper, we analyze the stress behavior of a chiral amino acid, alanine, adsorbed on Cu(110) from first-principles calculations. In particular, we focus on the alanine (2×3) phase. One question of interest is how will the stress be affected by the "molecular chirality," associated to the chiral center in alanine (i.e., to the distinction between R and S enantiomers), and by the "footprint chirality," associated to the bonding geometry.[22] Upon adsorption on Cu(110), alanine deprotonates to yield a carboxylate group and adopts a three-point binding through the O and N atoms. The two O atoms lie on neighboring Cu sites along $[1\bar{1}0]$, and the N atom lies at either of the next Cu atoms in close-packed row (i.e., there are two possible sites for N atoms that give rise to two different footprints) with the methyl group at the bridge pointing out of the surface (see Fig. 1). This adsorption geometry has been well documented using variety of techniques, which include DFT,[23,24] photoelectron diffraction (PhD),[25] x-ray photoelectron spectroscopy (XPS),[24,26] reflec-

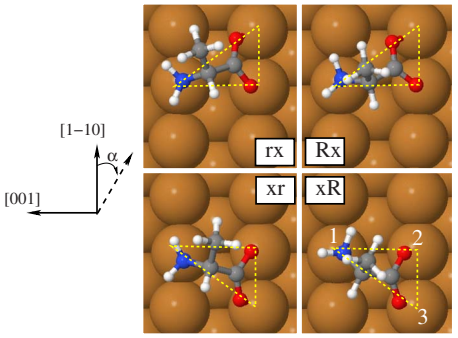

FIG. 1. (Color online) (2×3) unit cell of $\Theta=1/6$ models. The color code for the atoms is white=H, gray=C, blue (left)=N, and red (right)=O. The three point binding footprint in each case is schematically represented by dashed triangles. The left-hand side inset shows the sign convention adopted here for a positive α value, with the eigenvector $\hat{v}_1$ depicted as a dashed line.

 ©2010 The American Physical Society

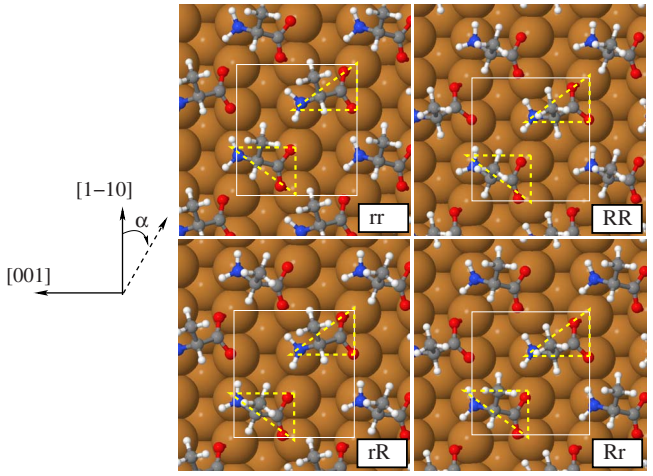

FIG. 2. (Color online) $\Theta = 1/3$ enantiopure models. The solid rectangle shows the (2×3) unit cell and footprints are indicated with dashed triangles.

tion absorption infrared spectroscopy,[26] and near-edge x-ray absorption fine structure (NEXAFS).[24]

In enantiopure alanine adsorption, molecular assembly occurs at high coverage and three phases appear at temperatures 300, 430, and 470 K. Up to 470 K, assemblies are homochiral[48] and defined clusters (hexamers) can be observed at the intermediate temperature phase by scanning tunneling microscopy (STM).[26,27] However, the high temperature phase shows an *achiral* organization, yet ordered within islands, that yields a (2×3) low-energy electron diffraction (LEED) pattern with missing spots, implying glide symmetry of some kind.[26] At this saturation coverage phase, $\Theta = 1/3$, there are two molecules per unit cell (see Fig. 2). However, if only the footprint chirality of the molecule is considered, pseudoglide symmetry arises when the two molecules in the unit cell have different footprints. DFT calculations show an energy minimum for such configuration.[23] Since the two molecules have different methyl group orientations and intramolecular scattering is weaker than adsorbate-metal interaction, the latter will be dominant in electron diffraction, as observed in PhD experiments.[25]

The scenario is equally inconclusive if racemic mixtures of R and S alanine are considered. In this case, the (2×3) LEED pattern with missing spots is recovered at high coverages, islands appear and full periodicity is not achieved.[28] It had been previously predicted theoretically that, as there is no significant difference between the adsorption energies of enantiopure and racemic (2×3), segregation of enantiopure domains will not happen.[23]

The question that arises here is what surface properties are sensitive enough to molecular chirality. Such information is crucial to characterize unexpected pseudoachirality in situations like the one above or to quantify the degree of enantiomer segregation when depositing a racemic mixture. Having this in mind, circular dichroism in the angular dependence (CDAD) of photoemission has been measured for Cu(110)/alaninate by Polcik *et al.*[29,30] However, the chiral effect on CDAD attributed to molecule chirality is ~1% only, much weaker than the effect of a chiral experimental setup.

In the present paper we analyze, using DFT calculations, the ability of surface stress to crossover the sensitivity limit between molecular and footprint chirality in Cu(110)/alaninate. This system provides a suitable benchmark, where we have studied the low- and high-coverage regimes, and the behavior of enantiopure and racemic mixtures.

II. CALCULATIONS

The DFT calculations were performed using plane-wave basis sets to span the electronic wave functions as implemented in CASTEP,[31] ultrasoft pseudopotentials to describe the ion cores[32] and the generalized gradient approximation (GGA) for the exchange and correlation functional in the Perdew-Wang formulation.[33] The reciprocal space was sampled using Monkhorst-Pack (MP) meshes,[34] and the cutoff energy for the basis set was 340 eV. The calculated bulk Cu nearest-neighbor distance is 2.550 Å. The surfaces were modeled by finite slabs in the supercell approach, containing eight Cu layers and the equivalent to six layers of vacuum. Convergence criteria for the ground state was 10^{-7} eV/atom. Equilibrium geometries were found by minimizing both the total energy and the forces on individual atoms with tolerances 10^{-5} eV and 10^{-3} eV/Å, respectively. Some of the structures proposed in Refs. 24 and 35 were used as the starting point for geometry optimization. The adsorbates and the outer four Cu layers were allowed to relax. Atomic positions were converged within 10^{-3} Å. In the enantiopure model calculations, the R-alaninate enantiomer was used. For the (2×3) reconstruction, a $3\times3\times1$ MP mesh was used to determine the equilibrium adsorption geometries. No spin-polarized ground states were found. Subsequently, the surface stresses in those geometries were obtained with a more accurate basis set of 390 eV energy cutoff and a $12\times12\times1$ MP mesh, which was found to provide suitably converged values.[49] Three structures in larger cells were also examined that required a $12\times6\times1$ MP grid.

CASTEP calculates the three-dimensional stress in the supercells at their ground state, $\vec{\vec{\tau}}$, from the Hellman-Feynman theorem, where the strain derivatives in the energy functional follow from the stress theorem of Nielsen and Martin.[4–6] The two-dimensional surface stress induced by adsorption, $\overleftrightarrow{\Delta\sigma}$, was obtained by doing

$$\overleftrightarrow{\Delta\sigma} = c(\vec{\vec{\tau}}^{\mathrm{Cu(110)/ala}} - \vec{\vec{\tau}}^{\mathrm{Cu(110)}}), \quad (1)$$

where c is the supercell height and $\vec{\vec{\tau}}^{\mathrm{Cu(110)/ala}}$ and $\vec{\vec{\tau}}^{\mathrm{Cu(110)}}$ are the in-plane components of the three-dimensional stress calculated in the alaninate/Cu(110) system supercell and in a clean relaxed Cu(110) slab, respectively. The calculations on the two slabs were performed on supercells of equal sizes and keeping identical basis sets in order to minimize numerical errors.

The tensor $\overleftrightarrow{\Delta\sigma}$ can be written as a 2×2 matrix. In the following, we will denote its eigenvalues as $\Delta\sigma_1$ and $\Delta\sigma_2$, such that $|\Delta\sigma_1| > |\Delta\sigma_2|$. The asymmetry will be quantified by the angle α between $[1\bar{1}0]$ and the eigenvector $\hat{v}_1$ associated to $\Delta\sigma_1$, such that a positive (negative) value indicates clockwise (anticlockwise) rotation from $[1\bar{1}0]$ as described in Fig.

1. The choice of MP mesh yields error bars of 0.001 eV Å^{-2} and 6×10^{-5} eV Å^{-2} in diagonal and extradiagonal terms of $\overleftrightarrow{\Delta\sigma}$, that would propagate into error bars for $\hat{v}_1$ direction of $\lesssim0.8°$ at low coverage ($\Theta=1/6$) and $\lesssim0.2°$ at medium-high coverage stress matrices, respectively. Due to the presence of oxygen species, the cut-off energy needs to be raised up to 390 eV in order to achieve error bars of the same order in the $\overleftrightarrow{\Delta\sigma}$ components and in α.

Convergence with respect to the number of substrate layers is less critical here than when calculating intrinsic stresses, as the $\overleftrightarrow{\Delta\sigma}$ tensor is mainly contributed by the molecule-substrate interaction, and this interaction is sufficiently converged for the chosen slab thickness. The intrinsic surface stress of clean Cu(110) was determined using a symmetric slab of 14 layers (allowing for a vacuum gap equivalent to ten layers), where four layers were relaxed at both ends of the slab. A $20\times28\times1$ MP grid was used for (1×1) surface periodicity.[50] The spurious contribution of the bulklike part of the slab was removed following the method described in Ref. 7. Values of $\sigma_{[1\bar{1}0]}=0.086$ and $\sigma_{[001]}=0.049$ eV Å^{-2} are found (the values reported from DFT calculations within the local-density approximation are 0.096 eV Å^{-2} and 0.090 eV Å^{-2}, respectively[36]).

Since alanine dehydrogenates upon adsorption, adsorption energies per molecule, E_{ads}, were calculated from

$$E_{ads}=\frac{1}{N}(E_{\mathrm{ala/Cu(110)}}-E_{\mathrm{Cu(110)}})-E_{\mathrm{ala,gas}}+\frac{1}{2}E_{\mathrm{H_2,gas}}, \quad (2)$$

where N is the number of alaninate species per unit cell and the four E terms in the right-hand side correspond to the total energies of the alaninate/Cu(110) slab, the clean Cu(110) slab with the same unit cell, an alanine molecule in the gas phase, and a H_2 molecule, respectively. Equation (2) yields adsorption energies with gas-phase molecules as a reference. The relative stabilities of different adsorption geometries are identical regardless of the chosen reference. The calculations involving the gas phase molecules were made in a $12\times12\times12$ Å^3 supercell.

III. RESULTS

Calculations have been carried out for a number of adsorption models proposed in the literature, both homochiral and heterochiral. For enantiopure models, R alanine is chosen. Due to the symmetry of the fcc (110) surface, S alanine provides the same results, except that $\overleftrightarrow{\Delta\sigma}$ is mirror flipped. All $\overleftrightarrow{\Delta\sigma}$ and E_{ads} values are summarized in Table I.

TABLE I. Principal stresses and orientations of the adsorption models discussed herein. The last column shows the adsorption energies per alanine molecule.

Model	$\Delta\sigma_1$ (eV Å^{-2})	$\Delta\sigma_2$ (eV Å^{-2})	α (deg)	E_{ads} (eV)
xR	−0.060	−0.011	11.1	−1.29
Rx	−0.061	−0.004	−17.4	−1.13
xr	−0.052	0.001	15.9	−1.09
rx	−0.058	−0.009	−13.5	−1.12
rr	−0.136	−0.063	−2.9	−1.42
RR	−0.140	−0.048	−4.9	−1.42
rR	−0.144	−0.055	−2.4	−1.44
Rr	−0.147	−0.059	−3.6	−1.44
RS	−0.142	−0.065	−0.1	−1.34
Rs	−0.128	−0.051	1.0	−1.40
rs	−0.141	−0.069	−1.9	−1.42
SR	−0.154	−0.057	2.3	−1.43
sR	−0.148	−0.056	−4.1	−1.45
sr	−0.140	−0.055	−2.7	−1.46
RrR	−0.110	−0.044	−3.1	−1.44
RsR	−0.114	−0.043	−1.2	−1.46

A. Θ=1/6 models

Models with coverage $\Theta=1/6$, containing one alaninate per (2×3) unit cell, describe isolated monomer adsorption and account for the disordered adlayer found at low coverage.[26] According to Ref. 24, there are four possible adsorption geometries, depicted in Fig. 1 and labeled xR, Rx, rx, and xr. In the notation used here, "R" and "r" configurations account for the two types of monomer distortion caused by adsorption: in R configuration the molecule backbone is bent and the methyl group points outwards nearly perpendicular to the surface and in the r configuration the molecule backbone is linear and the C-CH_3 bond has a large in-plane component. The position of the "x" label accounts for the three-point footprint type.

From the DFT analysis only, these four models are equally plausible, since they yield similar E_{ads}. In all models, $\overleftrightarrow{\Delta\sigma}$ is highly anisotropic with $\hat{v}_1$ lying close to the substrate mirror plane along $[1\bar{1}0]$. Stress magnitudes are similar for all models with $\Delta\sigma_1\sim-0.06$ eV Å^{-2}, i.e., compressive and a smaller $\Delta\sigma_2\sim-0.01$ eV Å^{-2}. The misalignment takes values $\sim15°$, where the sign (see Fig. 1) depends on the footprint.

At this coverage, monomers are isolated in the sense that there exists no H bonding between adjacent monomers, not even along the [001] direction. To confirm this point, an extra calculation was made for the xR geometry in a (3×3) supercell that changes the E_{ads} only by $\lesssim0.02$ eV and shows $\alpha=11.7°$, in agreement with the value found for the (2×3) xR model. $\Delta\sigma_1$ and $\Delta\sigma_2$ are smaller in magnitude, as expected from coverage reduction, taking values of −0.038 eV Å^{-2} and −0.008 eV Å^{-2}, respectively.

B. Θ=1/3 models

The $\Theta=1/3$ models are representative of the experimentally observed pseudo-ordered (2×3) phases. The two alaninate molecules in the unit cell are constrained to have opposite footprints. Figure 2 shows the four possible combinations of homochiral monomer geometries, labeled Rr, rR, RR, and rr. $\overleftrightarrow{\Delta\sigma}$ is compressive and strongly anisotropic with $\Delta\sigma_1\sim-0.14$ eV Å^{-2}, $\Delta\sigma_2\sim-0.055$ eV Å^{-2} and $\hat{v}_1$ oriented close to $[1\bar{1}0]$ with $|\alpha|\lesssim5°$ and rotated anticlock-

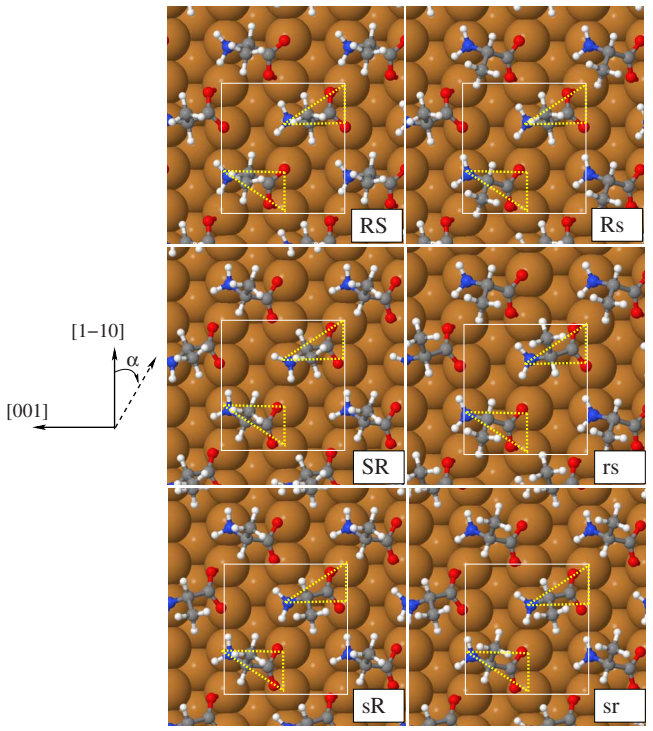

FIG. 3. (Color online) $\Theta=1/3$ racemic models. The solid rectangle shows the (2×3) unit cell and footprints are indicated with dashed triangles.

wise. The molecular overlayer is stabilized by H bonds, and therefore E_{ads} values are larger than in the low-coverage models. However, from the DFT analysis only, these four models are plausible, since they yield similar E_{ads}. Since only rr and Rr models agree with experimental XPS and NEXAFS data, the other two have been disregarded.[24]

We have also considered racemic $\Theta=1/3$ models, containing one R alanine and one S alanine per unit cell. This results in six possible combinations, RS, Rs, rs, SR, sR, and sr, shown in Fig. 3 and Table I. The $\overleftrightarrow{\Delta\sigma}$ features resemble those of the enantiopure models, except that both positive and negative α values are found. Again, similar E_{ads} values make it difficult to single out a most probable geometry.

C. $\Theta=3/10$ models

Another enantiopure model with medium coverage $\Theta=3/10$, labeled as RrR, has been studied that possesses a $\begin{pmatrix}5 & -1\\ 0 & 2\end{pmatrix}$ unit cell (see Fig. 4). This periodicity contains islands of (2×3) meshes with opposite footprints inside. Footprint rows are alternated such that, overall, the two types are present in a 2:1 ratio. RrR has the smallest unit cell in the $\begin{pmatrix}(3n+2) & -1\\ 0 & 2\end{pmatrix}$ family of surfaces, that produce a rather dense packing of molecules but allow different footprint proportions. In LEED experiments this reconstruction will be manifest as additional superstructure spots. Since it contains short-range (2×3) ordering, only the spots lying close to the (2×3) reconstruction spots in the reciprocal space will be visible on the LEED pattern, so this model can account for the small deviations in some spot positions[37] that can be

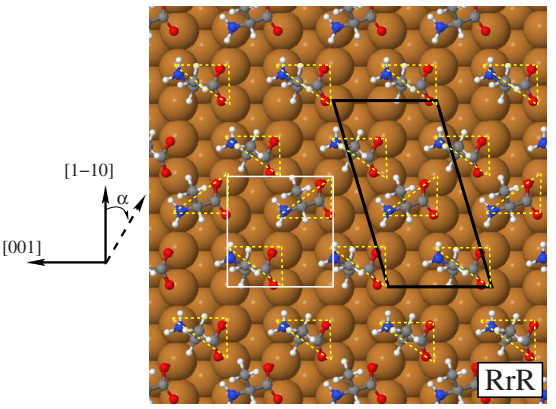

FIG. 4. (Color online) RrR model. The pseudo-(2×3) cell is shown in white and the real oblique cell in black.

observed in Fig. 12 of Ref. 26. The electrons scattered by different (2×3) domains in antiphase also yield the usual experimentally observed $(m\pm1/2,0)$ spot extinctions.

A weak anticlockwise rotation of $\alpha=-3.1°$ is found for the RrR model, consistent with the negative α values found in $\Theta=1/3$ R-alanine models. Finally, the enantiomeric effect at medium coverage has been tested with the model RsR, that consists in replacing the central molecule in the unit cell of Fig. 4 by its mirror image. This produces an even weaker $\alpha=-1.2°$. In both cases, $\Delta\sigma_1\sim-0.11$ eV Å^{-2} and $\Delta\sigma_2\sim-0.04$ eV Å^{-2}.

IV. DISCUSSION

For $\Theta=1/6$, the stress induced upon adsorption depends strongly on the footprints, and asymmetries happen clockwise or anticlockwise depending on the footprint chirality of the adsorbate (see Table I and Fig. 1). However, the influence of the methyl-group orientation or the molecule backbone bending seem to be negligible, hence molecular chirality does not greatly influence the stress in this case. The major principal stress, $\Delta\sigma_1$, is compressive, qualitatively consistent with negative charge being transferred from the Cu substrate to the molecule[2,10] [although some exceptions to this argument exist, e.g., H/Pt(111) (Refs. 38 and 39)]. A Bader analysis of the charge distribution[40] in the clean surface and the $\Theta=1/6$ models shows that the three Cu atoms bound to the molecule donate electrons, while the others remain unaffected. Stress release is therefore localized. For example, charges removed from the Cu atoms 1, 2, and 3 in model xR (see Fig. 1) are 0.10, 0.31, and 0.24 electrons, respectively. Thus, different amounts of charge are removed from every other Cu row and the symmetry of the substrate charge distribution is lowered. Figure 5 shows, for the xR model, the projected density of states (DOS) on the Cu(1–3) atoms and the alaninate species. The gas phase alanine levels are also shown as a reference. The electrons donated by the Cu atoms populate the half-filled energy levels in the alaninate species so that the highest occupied molecular orbital levels, now broadened by adsorption, lie below the Fermi level, E_F, and the lowest unoccupied molecular orbital can be distinguished at ~2 eV above E_F.

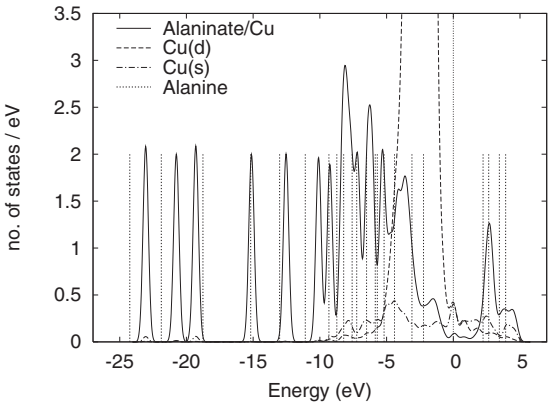

FIG. 5. Projected DOS on the alaninate species (solid line) and on the *d* and *s* orbitals of the Cu(1–3) atoms (dashed and dashed-dotted lines, respectively) in the xR model. The surface Fermi level is at $E_F=0$. The dotted lines show the gas-phase alanine discrete energy levels, also with $E_F=0$.

In the low-coverage noninteracting regime, molecules adopt disordered adsorption sites. The monomer E_{ads} values for xR, Rx, xr, and rx models are −1.29 eV, −1.13 eV, −1.09 eV, and −1.12 eV, respectively (see Table I), lying within the DFT error limits for E_{ads} calculations. Thus, it cannot be ensured that there will be a preferred monomer configuration and no segregation into domains is expected. Thus, if a low-coverage racemic mixture was deposited on the surface, no effect associated with molecular chirality would be observed, since $\overleftrightarrow{\Delta\sigma}$ behavior would be dominated by the aforementioned footprint chirality. In a biased situation where adsorbates with footprints of type xR or xr (Rx or rx) were present in excess, a stress asymmetry would be induced clockwise (anticlockwise) with respect to $[1\bar{1}0]$ (see Fig. 1) with an intermediate angle $0 \lesssim \alpha \lesssim 15°$ $(-15° \lesssim \alpha \lesssim 0)$.

In the high-coverage regime, the $\Theta=1/3$ condition imposes the constraint that two molecules with different footprints must fit in the (2×3) unit cell, for both enantiopure and racemic cases. Although it is not imposed by the surface symmetry in any of the studied cases, this geometrical feature dilutes the $\hat{v}_1$ deviation from $[1\bar{1}0]$ seen at low coverage. A Bader analysis has been carried out for model sr. The two rows in the unit cell contribute approximately the same charge, as all the rows support two O atoms and one N atom per unit cell. Charges transferred into molecule *A* from the Cu (1–3) atoms are 0.13, 0.27, and 0.32 electrons, respectively (see Fig. 6). In molecule *B*, Cu (4–6) atoms transfer 0.12, 0.23, and 0.19 electrons, respectively.

The same analysis in the rr model provides very similar values of 0.11, 0.25, and 0.31 electrons for Cu (1–3), respectively, and 0.14, 0.27, and 0.18 electrons for Cu (4–6), respectively (see Fig. 6). Thus, charge is being removed from all Cu atoms at the surface outer layer and electron transfer into individual N and O atoms is similar to that found at low coverage. This is consistent with an increasingly compressive $\overleftrightarrow{\Delta\sigma}$. In the $\Theta=1/3$ models, we find $\Delta\sigma_1 \sim -0.14$ eV Å^{-2}, a magnitude about 2.5 times larger than that of the $\Theta=1/6$ models, and $\Delta\sigma_2 \sim -0.055$ eV Å^{-2}, as shown in Table I. Thus, the system is outside the linear regime, since coverage proportionality is not held by $\Delta\sigma_1$ (see Fig. 7). Furthermore, the $\Delta\sigma_2$ compressive character is no longer non-negligible at medium-high coverages, consistent with an increasing lateral interaction between alaninate monomers along [001].

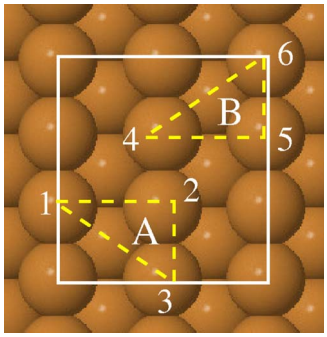

FIG. 6. (Color online) Labeling of Cu atoms in the $\Theta=1/3$ models unit cell.

At saturation coverage, weak intermolecular interactions, albeit non-negligible for stress relief, are present. These interactions happen via H bonding plus a small repulsive non-H-bonding interaction that may cause some destabilization due to steric hindrance of the methyl group.[41] GGA functionals are found to provide an insufficient description of some intermolecular H-bonding systems, e.g., water hexamers, since they do not account for dispersion (i.e., van der Waals) interactions.[42] Recent progress in this area includes semiempirical corrections[42] and the development of van de Waals exchange and correlation functionals.[43,44] The DFT-GGA calculations made in the present work can satisfactorily account for 80–90 % of the actual bonding interaction found in gas-phase alanine dimers experimentally and by the quantum chemical MP2 formalism.[41] For alaninate on Cu(110), overall stabilization by increasing the coverage from 1/6 to 1/3 is on average 0.26 eV per molecule (see adsorption energies in Table I). The H-bond contribution obtained from a topologi-

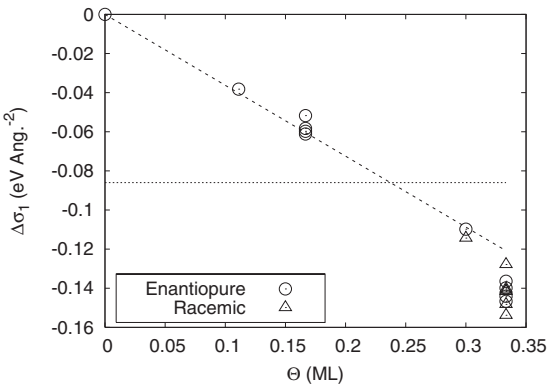

FIG. 7. Compilation of the major principal stress difference, $\Delta\sigma_1$, as a function of coverage Θ for the 17 models studied in this work. Enantiopure and racemic models are represented by circles and triangles, respectively. A linear scaling is observed up to $\Theta=0.3$. The horizontal line indicates when tensile stress along $[1\bar{1}0]$ in clean Cu(110) would be relieved.

cal analysis of the electron density is 1.0–1.4 eV per cell in the $\Theta=1/3$ models.[41] Most H bonds in the adlayer are NH$\cdots$O, i.e., oriented close to $[1\bar{1}0]$. In the three NH$\cdots$O H bonds of a S-alanine molecular crystal, the experimental NH$\cdots$O bond lengths are 1.92 Å, 2.00 Å, and 1.91 Å and the respective angles are 166°, 157°, and 170°.[45] The $\Theta=1/3$ structures have four H bonds per unit cell and all their bond lengths lie close to 2 Å, but the angles are typically 20° smaller than those of crystalline alanine (they can be as small as 130°). Therefore, NH$\cdots$O bonds would benefit from a slight expansion of the Cu substrate along $[1\bar{1}0]$, which enhances the observed compressive $\Delta\sigma_1$ value and produces the nonlinear increase with coverage.

Homochiral (2×3)-periodic adlayers of R alaninate at saturation coverage show anticlockwise rotation of $\hat{v}_1$ for all configurations in the range $2.5°-5°$, as shown in Table I. Therefore, the surface stress captures the molecular chirality of R alaninate (or S alaninate) on Cu(110), although it is insensitive to a heterochiral alanine adlayer.

The RrR model is an interesting case study, since it presents an imbalance of footprints but is yet enantiopure. Since 2/3 of the molecules show xR-like footprints, a clockwise deviation of $\hat{v}_1$ would be intuitively predicted. However, the calculations yield a negative $\alpha=-3.1°$. This can be interpreted as a consequence of the intermolecular interactions. The islands containing Rr and rR ordering, stabilized by H bonds, are the main contribution to the net $\overleftrightarrow{\Delta\sigma}$ in RrR. Weaker H bonds of 2.17 Å bind together distant xR molecules. Regarding magnitudes, the major principal stress, $\Delta\sigma_1=-0.11$ eV Å^{-2}, is an intermediate value between $\Delta\sigma_1\sim-0.06$ eV Å^{-2} and $\Delta\sigma_1\sim-0.14$ eV Å^{-2} of $\Theta=1/6$ and $\Theta=1/3$ models, respectively. If an enantiomeric excess is created by mirroring one of the molecules as in model RsR, the angular deviation is reduced to $\alpha=-1.2°$. These two stress models show that intermolecular interactions prevail at medium coverage, masking both footprint and enantiomeric effects.

It has been proposed that stress relief might be behind the formation of regular alanine hexamer assemblies.[27] STM reveals well-defined channels between haxamer rows with a global $\begin{pmatrix}5 & -3\\ 2 & 2\end{pmatrix}$ periodicity. These channels along the $[1\bar{1}2]$ direction create a chiral long-range dominating structural feature. From Fig. 7 and bearing in mind that the intrinsic stress in Cu(110) is 0.086 eV Å^{-2} along $[1\bar{1}0]$ and 0.049 eV Å^{-2} along [001], the system would be entering a net compressive stress scenario at $\Theta\gtrsim1/4$, when adsorbates begin to form a H-bound network. Some of that net stress may be partially relieved by breaking a few H bonds and reducing Θ locally through the observed clustering into hexamers. Unfortunately, DFT modeling of such clustering would be daunting because of the large unit-cell sizes involved. A related example is found in the case of phthalocyanines on Ag(111), where the molecule-substrate interaction is weak, a H-bond deformation reduces the lattice mismatch between the SAM and the substrate, and therefore it reduces the stress.[46]

We have shown that asymmetries introduced in the surface stress by chemisorption of chiral species at low-coverage regimes depend mainly on the adsorption footprint. Amino acids seem to offer a range of possibilities, as the footprint can be tunned by replacing the methyl group by a chain of general formula $CH_2(CH_2)_xG$, where $x=\{0,\ldots,n\}$ and G is a functional group that can chemisorb on the metallic substrate. Based on this argument, an adsorbate with achiral footprint, e.g., (R,R)-tartaric acid on Cu(110),[47] would not show a strong asymmetry. Any observed asymmetry in that case would be an effect of the assembly of molecules. In the (2×3) alaninate/Cu(110) cases shown here with non-negligible $\alpha\gtrsim5°$, the asymmetries are due to the adsorbate chirality, since the unit cell itself is achiral (it has rectangular shape).

V. CONCLUSIONS

Surface stress changes on adsorption of alaninate on Cu(110) are sensitive to footprint chirality in the low-coverage regime, and the principal stresses show a maximum $\sim15°$ deviation from the $[1\bar{1}0]$ mirror crystallographic direction. At the (2×3) phase saturation coverage, where both footprints are present in the unit cell and the intermolecular interactions (H bonds) are non-negligible, angular-deviation effects are reduced to a few degrees. We have shown that asymmetries of $2°-5°$ are observable in saturated enantiopure adlayers of alanine on Cu(110). Thus, surface stress orientation is weakly sensitive to molecular chirality, i.e., to monomer atomic geometry.

H bonding at saturation is strong enough to drive the system out of the low-coverage linear stress regime. An intermediate coverage regime, with footprint imbalance, has also been studied where the excess footprint does not correlate with the observed asymmetry. Instead, the existence of densely packed islands of molecules seems to dominate the stress orientation. The Cu substrate relieves most of its intrinsic tensile stress at $\Theta\gtrsim1/4$, precisely when H bonds appear between alaninate monomers, switching to compressive at higher coverage.

ACKNOWLEDGMENTS

Dirk Sander and Stephen J. Jenkins are warmly acknowledged for useful discussions. EPSRC is acknowledged for financial support and the Cambridge High Performance Computing Cluster *Darwin* for computing time. M.B.R. is grateful to the European Comission for funding through the Marie Curie Intra-European program.

*mb633@cam.ac.uk
†Present address: Johnson Matthey Technology Centre, Blounts Court, Sonning Common, Reading RG4 9NH, UK.

[1] R. Shuttleworth, Proc. Phys. Soc., London, Sect. A **63**, 444 (1950).
[2] H. Ibach, Surf. Sci. Rep. **29**, 195 (1997).
[3] P. Müller and A. Saúl, Surf. Sci. Rep. **54**, 157 (2004).
[4] O. H. Nielsen and R. M. Martin, Phys. Rev. Lett. **50**, 697 (1983).
[5] O. H. Nielsen and R. M. Martin, Phys. Rev. B **32**, 3780 (1985).
[6] O. H. Nielsen and R. M. Martin, Phys. Rev. B **32**, 3792 (1985).
[7] R. J. Needs, Phys. Rev. Lett. **58**, 53 (1987).
[8] R. J. Needs and M. J. Godfrey, Phys. Scr. **T19**, 391 (1987).
[9] P. J. Feibelman, Phys. Rev. B **50**, 1908 (1994).
[10] H. Ibach, J. Vac. Sci. Technol. A **12**, 2240 (1994).
[11] W. Haiss, Rep. Prog. Phys. **64**, 591 (2001).
[12] D. Sander, Rep. Prog. Phys. **62**, 809 (1999).
[13] D. Sander, Curr. Opin. Solid State Mater. Sci. **7**, 51 (2003).
[14] D. Sander, Z. Tian, and J. Kirschner, Sensors **8**, 4466 (2008).
[15] R. Berger, E. Delamarche, H. P. Lang, C. Gerber, J. K. Gimzewski, E. Meyer, and H.-J. Güntherodt, Science **276**, 2021 (1997).
[16] V. Srinivasan, G. Cicero, and J. C. Grossman, Phys. Rev. Lett. **101**, 185504 (2008).
[17] M. Blanco-Rey, S. J. Pratt, and S. J. Jenkins, Phys. Rev. Lett. **102**, 026102 (2009).
[18] D. Sander, A. Enders, and J. Kirschner, Europhys. Lett. **45**, 208 (1999).
[19] K. Dahmen, H. Ibach, and D. Sander, J. Magn. Magn. Mater. **231**, 74 (2001).
[20] H. L. Meyerheim, D. Sander, R. Popescu, J. Kirschner, O. Robach, S. Ferrer, and P. Steadman, Phys. Rev. B **67**, 155422 (2003).
[21] C. Bombis, M. Moiseeva, and H. Ibach, Phys. Rev. B **72**, 245408 (2005).
[22] S. M. Barlow and R. Raval, Curr. Opin. Colloid Interface Sci. **13**, 65 (2008).
[23] R. B. Rankin and D. S. Sholl, Surf. Sci. **574**, L1 (2005).
[24] G. Jones, L. B. Jones, F. Thibault-Starzyk, E. A. Seddon, R. Raval, S. J. Jenkins, and G. Held, Surf. Sci. **600**, 1924 (2006).
[25] D. I. Sayago, M. Polcik, G. Nisbet, C. L. A. Lamont, and D. P. Woodruff, Surf. Sci. **590**, 76 (2005).
[26] S. M. Barlow, S. Louafi, D. Le Roux, J. Williams, C. Muryn, S. Haq, and R. Raval, Surf. Sci. **590**, 243 (2005).
[27] S. M. Barlow, S. Louafi, D. Le Roux, J. Williams, C. Muryn, S. Haq, and R. Raval, Langmuir **20**, 7171 (2004).
[28] S. Haq, A. Massey, N. Moslemzadeh, A. Robin, S. M. Barlow, and R. Raval, Langmuir **23**, 10694 (2007).
[29] M. Polcik, F. Allegretti, D. I. Sayago, G. Nisbet, C. L. A. Lamont, and D. P. Woodruff, Phys. Rev. Lett. **92**, 236103 (2004).
[30] F. Allegretti, M. Polcik, D. I. Sayago, F. Demirors, S. O'Brien, C. L. A. Lamont, and D. P. Woodruff, New J. Phys. **7**, 109 (2005).
[31] S. J. Clark, M. D. Segall, C. J. Pickard, P. J. Hasnip, M. Probert, K. Refson, and M. C. Payne, Z. Kristallogr. **220**, 567 (2005).
[32] D. Vanderbilt, Phys. Rev. B **41**, 7892 (1990).
[33] J. P. Perdew, J. A. Chevary, S. H. Vosko, K. A. Jackson, M. R. Pederson, D. J. Singh, and C. Fiolhais, Phys. Rev. B **46**, 6671 (1992).
[34] H. J. Monkhorst and J. D. Pack, Phys. Rev. B **13**, 5188 (1976).
[35] G. Jones, Ph.D. thesis, University of Cambridge, 2006.
[36] S. Olivier, G. Tréglia, A. Sául, and F. Willaime, Surf. Sci. **600**, 5131 (2006).
[37] G. Held (private communication).
[38] P. J. Feibelman, Phys. Rev. B **56**, 2175 (1997).
[39] Z. Tian, D. Sander, N. N. Negulyaev, V. S. Stepanyuk, and J. Kirschner, Phys. Rev. B **81**, 113407 (2010).
[40] R. F. W. Bader, *Atoms in Molecules: A Quantum Theory* (Oxford University Press, Oxford, 1990).
[41] G. Jones, S. J. Jenkins, and D. A. King, Surf. Sci. **600**, L224 (2006).
[42] B. Santra, A. Michaelides, M. Fuchs, A. Tkatchenko, C. Filippi, and M. Scheffler, J. Chem. Phys. **129**, 194111 (2008).
[43] M. Dion, H. Rydberg, E. Schroder, D. C. Langreth, and B. I. Lundqvist, Phys. Rev. Lett. **92**, 246401 (2004).
[44] T. Thonhauser, V. R. Cooper, S. Li, A. Puzder, P. Hyldgaard, and D. C. Langreth, Phys. Rev. B **76**, 125112 (2007).
[45] H. J. Simpson, Jr. and R. E. Marsh, Acta Crystallogr. **20**, 550 (1966).
[46] V. Oison, M. Koudia, M. Abel, and L. Porte, Phys. Rev. B **75**, 035428 (2007).
[47] M. Ortega Lorenzo, C. J. Baddeley, C. Muryn, and R. Raval, Nature (London) **404**, 376 (2000).
[48] We use the term homochiral (heterochiral) as equivalent to enantiopure (racemic or mixed).
[49] The increase in the energy cutoff from 340 to 390 eV does not alter significantly the adsorption energies, which change by $\lesssim$0.02 eV, or the atomic positions, which change by $\lesssim$0.01 Å and $\lesssim$0.03 Å in low- and high-coverage models, respectively.
[50] Convergence in clean Cu has been monitored in a bulk modulus (B) calculation for Cu, resulting in B=143 GPa for a 20×20×20 MP grid and a 340 eV energy cutoff. B changes by $\lesssim$2 GPa when increasing these parameters.